# ANGULAR SPECTRUM ANALYSIS APPLIED TO UNDERCLADDING FLAWS AND DIPOLE PROBES

M. Riaziat and B.A. Auld

E.L. Ginzton Laboratory
Stanford University
Stanford, CA 94305

## I. INTRODUCTION

An important class of subsurface cracks occur in nuclear power plant pressure vessels. These pressure vessels, normally made of carbon steel, are protected by a layer of weld material applied directly onto the surface, leaving a highly inhomogeneous cladding with a rough surface and a very irregular interface. Subsurface cracks originate at the interface between the carbon steel walls of the pressure vessel and the protective cladding layer. The propagation is initially into the carbon steel and eventually into the cladding, and needs to be detected before reaching the surface (Fig. 1). The inhomogeneity of the cladding material and the irregular surfaces pose serious difficulties for ultrasonic detection. These difficulties are less critical for eddy current testing due to the fact that the layered structure of the cladding has more variation in its elastic properties than its electrical conductivity.

The work reported here addresses the interaction of eddy currents with cracks in both the carbon steel and the cladding layer. Two approaches are taken in this program. The one discussed in this paper is analytical, using near field scattering theories. This approach is applied to closed cracks originating at the interface. The other approach (not reported here) is numerical, using a three dimensional finite element code developed by W. Lord and coworkers at Colorado State University (Ida, 1984). The numerical calculations will be used as a check on the theory, and will be extended to the geometries where the interactions cannot be determined analytically. Finally, the question of probe type to be used is addressed. Categorizing the probes according to a dipole approximation of their fields, some general conclusions will be made about the overall performance of two different probe types.

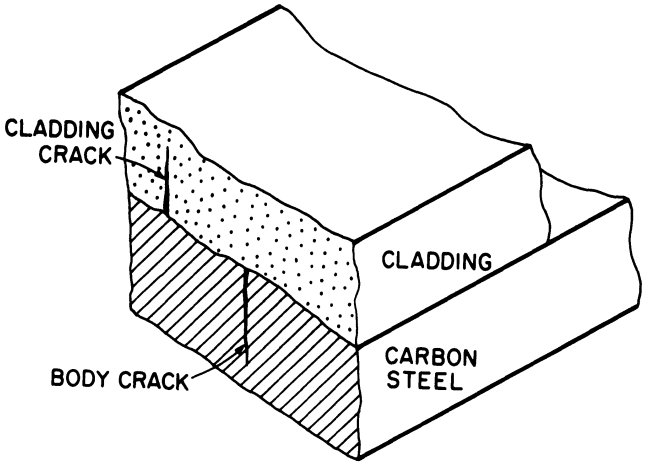


Figure 1
Subsurface Cracks in the Pressure Vessels in Nuclear Power Plants.

## II. SCATTERING CALCULATIONS

Most scattering theories in optics and radioscience deal with field expressions in the far field of the scatterer and can not be used to find the behavior of the evanescent fields close to the scattering object. One exception is the Sommerfeld scattering theory which can be used in certain simple geometries to find exact expressions for the scattered field both close to and far from the scatterer(Born and Wolf, 1980). In the scattering of eddy currents from cracks, this theory was first used successfully by Kahn et al. (1977), who applied it to closed two dimensional surface cracks in metals. We found the geometry of subsurface cracks in the pressure vessels also suitable for the application of this theory. We have been able to treat separately the cases of deep cracks either in the cladding material or in the carbon steel. (See Appendix for more detail.) For the uniform field contribution to the impedance change of the probe both cases yield expressions of the form

$$\Delta Z_p = \frac{2i}{\sigma_{cladd}} \left( \frac{H_0}{I} \right)^2 e^{-2d/\delta} C_p, \tag{1}$$

where $d$ is the distance of the crack tip from the surface, and $C_p$ is a number characterizing the crack. In the case of a crack in the cladding, $C_p$ is a constant independent of material properties given by

$$C_p = \int_0^1 \frac{\sqrt{1+\beta}}{\beta(1-\beta^2)}\, d\beta - \int_0^\infty \frac{\sqrt{1+i\beta}}{\beta(1+\beta^2)}\, d\beta, \tag{2}$$

which, when evaluated numerically, gives

$$C_p = 21.6\angle 0.7°. \tag{3}$$

For the crack into the carbon steel, the value of $C_p$ is not independent of the material properties and is given by,

$$C_p = \frac{2T(k=0)}{\pi} L_1(0) \int_0^\infty \frac{d\lambda}{\lambda^2 L_{1e}(\lambda)}. \tag{4}$$

$T(k=0)$ is the uniform field transmission coefficient at the interface between the cladding and the carbon steel, and the function $L_1$ is an algebraic expression depending on the material properties. The integral involved in the expression is well behaved and converges rapidly, and can therefore be evaluated numerically. A more detailed discussion of the scattering calculations is given in the Appendix.

## III. VERTICAL AND HORIZONTAL DIPOLES

No unique set of criteria exist for the categorization of eddy current probes, and the selection of probe type for most problems is usually done without any theoretical analysis. One simple method of categorizing probes is by their approximate field shapes. As can be seen in Fig. (2), most practical probes generate a field similar to that of a vertical dipole. Some other probes, such as the tape-head probe, have field shapes similar to that generated by a horizontal dipole. In order to be able to decide which of these two types are more suitable for general flaw detection it is instructive to evaluate the relative performances of horizontal and vertical dipoles.

The tangential magnetic fields due to dipoles of different orientations have closed form expressions in the spatial frequency domain. Specifically, for a dipole of general orientation, $(m = m_x\hat{x} + m_y\hat{y} + m_z\hat{z})$, a distance $z_0$ above a conductor with a reflection coefficient $\Gamma(k)$ the magnetic field spectrum is given by

$$h_t(k) = \hat{k}\frac{1-\Gamma}{4\pi}[ikm_z - k_x m_x - k_y m_y]e^{-kz_0}. \tag{5}$$

In order to compare the performances of vertical and horizontal dipoles, their responses to liftoff, and their sensitivities to flaws should be calculated.

Liftoff is most easily modeled as a change $\delta Z_s$ in the surface impedance of the test piece (Auld and Riaziat, 1983). This is demonstrated in Fig. (3). The impedance change $\Delta Z$ of the probe due to liftoff is then calculated in closed form utilizing Eq. (5).

$$(\Delta Z)_{liftoff} = \frac{1}{I^2} \int_{-\infty}^{+\infty} \int_{-\infty}^{+\infty} \delta Z_s(k) h_t^2(k)\, dk_x dk_y. \tag{6}$$

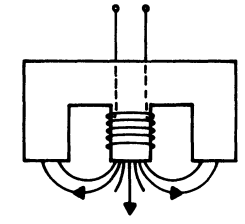

(a) VERTICAL

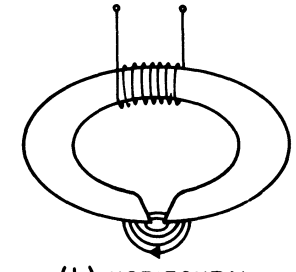

(b) HORIZONTAL

Figure 2

Two Ferrite-Core Probes with Fields Resembling Horizontal and Vertical Dipole Fields

The resulting expression for the impedance change of a dipole probe due to liftoff has the form

$$(\Delta Z)_{liftoff} = (2|m_z|^2 + |m_x|^2 + |m_y|^2)F(l,\omega), \tag{7}$$

where $F(l,\omega)$ is independent of probe parameters (Auld et al., 1983). It is seen from Eq. (7) that the sensitivity of a vertical dipole $m_z$ to liftoff variations is twice that of a horizontal dipole. This result has to be combined with a comparison of the relative sensitivities to flaws in order to make a conclusion about the overall performances.

The sensitivity of a probe to flaws is proportional to the square of its magnetic field tangential to the test piece surface, normalized with respect to the drive current. The peak signal magnitude is obtained when the point of maximum tangential field coincides with the position of the flaw. Therefore the normalized tangential magnetic field serves as a measure of probe sensitivity to flaws. When a horizontal dipole is placed a finite distance $z_0$ above a conducting plane, the maximum tangential field it generates happens directly underneath the dipole. The value of this field is easily evaluated when the plane is a perfect conductor,

$$|H_t|^2_{max} = |m_x/2\pi z_0^3|^2. \tag{8}$$

In the case of a vertical dipole, the tangential field vanishes at the projection point of the dipole on the surface. The maximum tangential field occurs a distance $z_0/2$ away from that point,

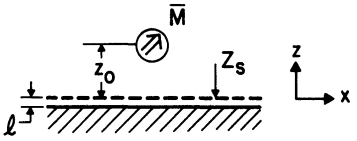


Figure 3
Liftoff Represented as a Surface Impedance Change

and is therefore, farther away from the dipole. The value of the maximum tangential field in this case is

$$|H_t|^2_{max} = 0.74|m_x/2\pi z_0^3|^2, \tag{9}$$

so the vertical dipole is seen to be more sensitive to the unwanted liftoff variations and less sensitive to the presence of the flaw. If we choose the ratio $\gamma = \Delta Z_{flaw}/\Delta Z_{liftoff}$ as a figure of merit characterizing the performance of the probe, it follows that the horizontal dipole performs better than the vertical dipole by a factor of 2.7.

In the above analysis of the shape of the tangential fields we assumed the metallic surface to be perfectly conducting. This assumption simplifies the calculations without altering the results significantly. To demonstrate this, inverse Fourier transforms of Eq.(5) were taken numerically for horizontal and vertical dipoles over imperfectly conducting substrates. The results are shown in Fig.(4). Note that the peak value of the field does not occur at the origin for the vertical dipole, and the ratio of the peaks is very close to what was calculated for a perfect conductor.

A point to be emphasized is that the dipole analysis presented here shows the superiority of a horizontal dipole field for flaw detection purposes. This argument should not be stretched to make conclusions about probes whose fields are far from dipole fields, such as large coils operating very close to a conducting plane. A conclusion that can be made from the foregoing analysis is that the field shape of a tapehead probe shown in Fig.(2) is more suitable for flaw detection than that of a cup--core probe. Experimental results on tapehead probes also point favorably to their use in flaw detection (Watjen and Bahr, 1984).

## IV. APPENDIX

Figure (A-1) shows the two dimensional geometry of a subsurface crack together with the path of the eddy currents around it. The crack is assumed to be closed and does not allow the passage of currents normal to its face. Both the cladding crack and the carbon steel crack are represented by the same picture, the only difference being the fact that for a crack in the carbon steel the material is not homogeneous across the $z = 0$ boundary.

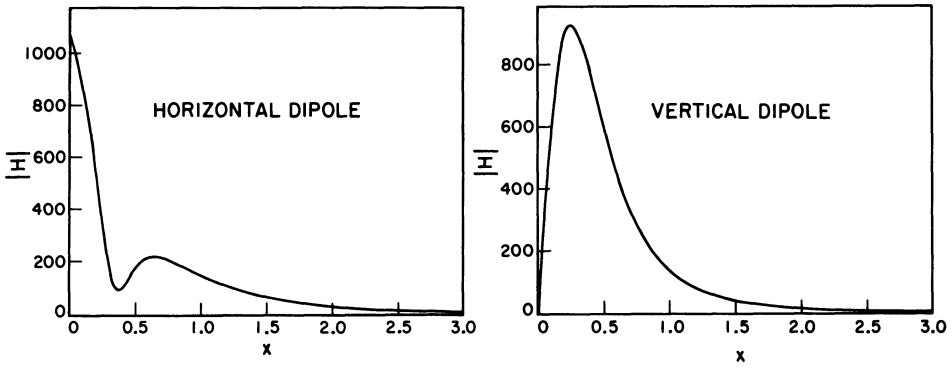


Figure 4

Tangential Magnetic Field for Vertical and Horizontal Dipoles (liftoff: 0.2 in, $\delta$: 0.02 in).

Since the interrogating field is quasistatic ($f < 10GHz$), the magnetic field within the crack is a constant. This constant depends on the depth of the crack, i.e., on the fraction of the eddy currents passing around the bottom of the crack. In fact, this constant contains all the information about the crack depth. As soon as the crack becomes deep enough so that all the eddy currents pass over its top, the magnetic field within the crack becomes zero, and no depth information can be collected by the probe. In the present treatment, it is assumed that the crack has indeed reached that critical depth, even though this assumption is not necessary. This constant value of the magnetic field in the crack is used as part of the necessary boundary conditions needed to solve the problem. The mathematical expressions for the boundary conditions will be given in the angular spectrum domain which is described below.

The electromagnetic field at a large distance from a source can be represented as the superposition of traveling plane waves ranging 180° in the angle of propagation.

$$H(r,\theta) = \int_0^{\pi} F(\cos\alpha) e^{-ik_0 r\cos(\theta\pm\alpha)} d\alpha. \qquad (A-1)$$

This description is not sufficient for the characterization of near field quantities due to the fact that in this region, evanescent waves are present that are not included in the above superposition. The evanescent waves can be represented by plane waves of

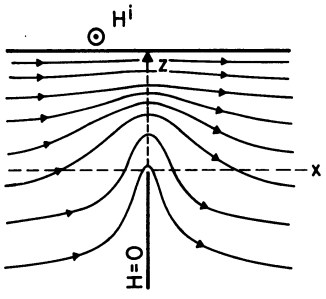


Figure A-1
The Path of Eddy Currents Around a Subsurface Crack

complex propagation angles which, when added to the range of Eq. (A-1), modify the integration limits to those of the contour $c$ in the complex $\alpha$ plane shown in Fig. (A-2). The quantity $F(\cos\alpha)$ is the angular spectrum of $H$, and defines the electromagnetic field completely. (The electric field is related to this by the characteristic impedance of the medium.)

This representation is closely related to the spatial frequency analysis (spatial Fourier transform). The relationship is seen explicitly when attention is focused on the field along one particular direction of $\theta$. For example, along the $x$ direction ($\theta = 0$), the magnetic field is

$$H(x) = \int_{-\infty}^{+\infty} \frac{F(\lambda)}{\sqrt{1-\lambda^2}} e^{-ik_0 x\lambda} d\lambda, \qquad (A-2)$$

where $\lambda = \cos\alpha$. In mapping from the $\alpha$ plane into the $\lambda$ plane the integration contour $c$ transforms to a path along the real axis (Fig. A-2), giving Eq. (A-2) the form of a spatial Fourier transform. This proves to be very convenient when calculating the probe response to the flaw, and comparing it to liftoff response which is easily formulated in the spatial Fourier domain (Auld and Riaziat, 1983).

Using Eq. (A-2) and the characteristic impedance of air $Z$, the tangential electric field along the same plane is found to be

$$E_x(x) = \int_{-\infty}^{+\infty} ZF(\lambda) e^{-ik_0 x\lambda} d\lambda. \qquad (A-3)$$

With the electric and magnetic fields written in the integral form we are now in a position to solve the boundary value problems.

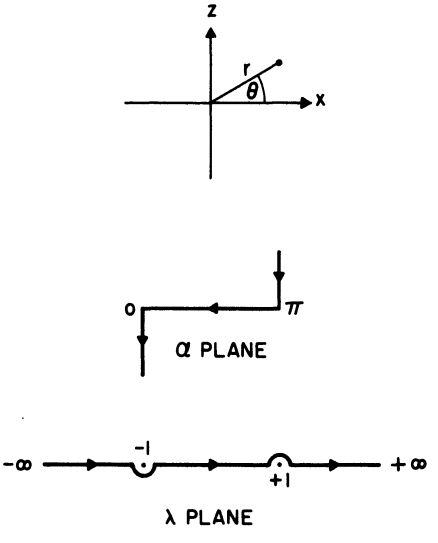


Figure A-2
Mapping From the $\alpha$ Plane into the $\lambda$ Plane

For the crack in the cladding, where there is no discontinuity in the material properties across the $z=0$ plane, two boundary conditions are imposed on the $yz$ plane; (i) The total magnetic field should vanish in the region $z<0$. In other words, in this region the scattered field should be equal and opposite to the incident field. (ii) Due to the symmetry of the scattered field no current flows along the $z$ axis in the region $z>0$. i.e., the scattered electric field has no $z$ component. These two conditions can be written as

$$\begin{cases} H^s + H^i = 0 & z<0 \\ E_z^s = 0 & z>0 \end{cases} \qquad (A-4)$$

If the incident field is a plane wave represented by $H_0 e^{ik_0\lambda_i^i z}$, Eq. (A-4) can be transformed into the angular spectrum domain to give

$$\begin{cases} \int F(\lambda) e^{-ik_0\lambda z} \frac{d\lambda}{\sqrt{1-\lambda^2}} = -H_0 e^{ik_0\lambda^i z} & z<0 \\ \int F(\lambda) e^{-ik_0\lambda z} d\lambda = 0 & z>0 \end{cases} \qquad (A-5)$$

This is a dual integral equation with $F(\lambda)$ as the unknown. A standard method for solving such equations is the Wiener--Hopf technique demonstrated in Fig. (A-3). The integration over the real axis is extended to a contour containing the upper half of the complex plane for the first integral and the lower half of the plane for the second integral. The residue theorem is then utilized to

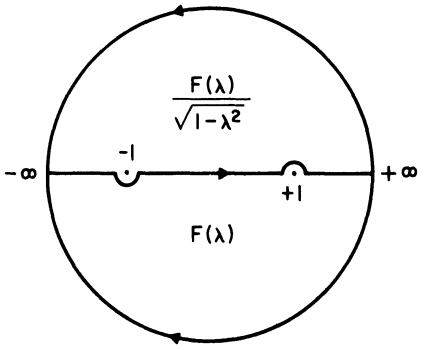


Figure A-3

The Wiener-Hopf Technique for the Solution of Dual Integral Equations

find a function with proper residues to satisfy the integrals. For the case of Eqs. (A-5) the function $F(\lambda)$ satisfying both equations turns out to be

$$F(\lambda) = -\frac{H_0}{2\pi i}\frac{\sqrt{1+\lambda^i}\sqrt{1+\lambda_z}}{\lambda_z+\lambda^i}. \qquad (A-6)$$

This expression, when integrated over all values of $(\lambda_z)$ gives the scattered field due to the presence of the flaw. This integration, however, is not necessary due to the fact that an eddy current probe responds only to those components in the spectrum that it can transmit. In particular, if a probe generates a uniform field $(k = 0)$, at the position of the flaw, it is only the $k = 0$ component of the scattered field that contributes to a change in its impedance. The impedance change of a probe in such a case is given by

$$\Delta Z_p = 2\sqrt{2\pi}\left(\frac{\omega\mu}{\sqrt{k_0^2 - k^{i2}}}\right)\left(\frac{H_0}{I}\right)\left[\frac{h^{s\prime}(k^i)}{I}\right], \qquad (A-7)$$

where $k^i$ is the spatial frequency of the incident field. The next step is combining Eqs. (A-6) and (A-7) which will finally yield the results given by Eqs. (1) and (2).

The case of a crack originating at the interface and propagating into the carbon steel is more involved and can not be treated using the method just described. Figure (A-4) shows the separation of this problem into two tractable scattering problems involving the interaction of a plane wave with a split impedance surface (Clemmow, 1966). The region of interest is the $z > 0$ half space.

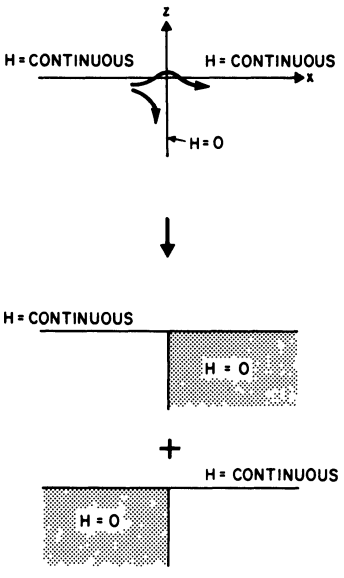


Figure A-4
The Separation of a Deep Interface Crack into Solvable Problems

Each one of the split impedance problems is reduced to a dual integral equation which is solved using the generalized Wiener--Hopf technique. This technique always involves the factorization of an algebraic function in the complex $\lambda$ plane into two functions $U(\lambda)$ and $L(\lambda)$ which are regular and without poles and zeros in the upper half plane and the lower half plane respectively. This can always be done in principle, but does not necessarily yield simple algebraic functions. For the uniform field excitation case, the result given in Eq. (4) involves the function $L_{1e}(\lambda)$ which is obtained by factorization. $L_{1e}(\lambda)$ is the even part of the function $L_1(\lambda)$ given by

$$L_1(\lambda) \approx \sqrt{1+\lambda}\exp\left\{\frac{i}{\pi}\cos^{-1}\lambda\tan^{-1}\frac{\gamma}{\sqrt{1-\lambda^2}}\right\}, \qquad (A-8)$$

$$\gamma = (1-i)(3.1)10^{-6}.$$

As can be seen, the expression $[\lambda^2 L_{1e}(\lambda)]^{-1}$ is well behaved and the integral in Eq. (4) can be evaluated numerically.

## V. REFERENCES

Auld, B.A., Muennemann, F.G., Riaziat, M., 1983, Quantitative modelling of flaw response in eddy current testing, to appear in: "Researc Techniques in Nondestructive Testing," R.S. Sharpe, ed., Academic Press, London.

Auld, B.A. and Riaziat, M., 1983, Spatial frequency analysis and matched filtering in electromagnetic NDE, J. Appl. Phys., 54:3509.

Born, M. and Wolf, E., 1980, "Principles of Optics," 6th ed., pp 556-591. Pergamon Press, Oxford.

Clemmow, P.C., 1966, "The Plane Wave Spectrum Representation of Electromagnetic Fields," Pergamon Press, Oxford.

Ida, N., 1984, Development of a 3-D eddy current model for non-destructive testing phenomena, to appear in: "Review of Progress in Quantitative Nondestructive Evaluation," 3, D.O. Thompson and D.E. Chimenti, eds., Plenum, New York and London.

Kahn, A.H., Spal, R. and Feldman, A., 1977, Eddy current losses due to a surface crack in conducting material, J. Appl. Phys., 48:4454.

Watjen, J.P. and Bahr, A.J., 1984, Evaluation of an eddy current tape-head probe, to appear in " Review of Progress in Quantitative Nondestructive Evaluation," 3, D.O. Thompson and D.E. Chimenti, eds., Plenum, New York and London.

## VI. ACKNOWLEDGEMENTS

This work was supported by the Electric Power Research Institute through the contract No. RP--1395--3, and by the National Bureau of Standards through the grant No. NB82--NAHA--3015.